

Determining the optimal standard test condition correction procedure for high-throughput field *I*-*V* measurements of photovoltaic modules

Yogeswara Rao Golve^{1,2}  | Anil Kottantharayil^{1,2}  | Juzer Vasi^{1,2} | Narendra Shiradkar^{1,2} 

¹National Centre for Photovoltaic Research and Education (NCPRE), Indian Institute of Technology Bombay, Mumbai, Maharashtra, India

²Department of Electrical Engineering, Indian Institute of Technology Bombay, Mumbai, Maharashtra, India

Correspondence

Narendra Shiradkar, National Centre for Photovoltaic Research and Education (NCPRE), Indian Institute of Technology Bombay, Mumbai, Maharashtra 400076, India.
 Email: naren@ee.iitb.ac.in

Funding information

Ministry of New and Renewable Energy of the Government of India, Grant/Award Number: 31/09/2015-16/PVSE-R&D

Abstract

The field-measured current-voltage (*I*-*V*) curves of photovoltaic (PV) modules need to be corrected to Standard Test Conditions (STC) in order to estimate the degradation rates. STC correction procedures have various attributes such as accuracy, requirement of minimum number and types of *I*-*V* curves, required irradiance range, and the type of correction (specific points or entire *I*-*V* curve) that determine their optimality for specific applications. This paper presents the investigation of accuracy and constraints of six different STC correction procedures for high-throughput field *I*-*V* measurements through experimental and simulation studies. Following STC correction procedures are considered in this paper: IEC 60891-Procedure 1, IEC 60891-Procedure 2, Modified IEC 60891-Procedure 1, Standard Irradiance and Desired Temperature (SIDT) procedure, Anderson procedure, and Voltage-Dependent Temperature Coefficient (VDTC) Procedure. Eight different simulation models for predicting the performance of PV modules at arbitrary irradiance and temperature are compared, and the simulation model that yields lowest root mean square error and the most accurate estimation of power temperature coefficient is identified. The simulated *I*-*V* curves using this model and the experimentally measured *I*-*V* curves on a flash tester at different temperatures and irradiances are provided as an input to all of the STC correction procedures. The average percentage errors in correction of maximum power (P_{max}), open-circuit voltage (V_{oc}), short-circuit current (I_{sc}), and fill factor (FF) were determined as a function of irradiance and temperature during measurement. Systematic biases introduced during correction by certain procedures were also identified. Based on the error estimation, constraints of various procedures, and requirements of high-throughput field *I*-*V* measurements, the most optimal STC correction procedure was identified. Moreover, the analysis of the root cause of superior performance of this procedure is also presented.

KEY WORDS

average percentage error, correction, current-voltage characteristics, equivalent cell temperature, experiment, fill factor, maximum power, open-circuit voltage, photovoltaic module, short-circuit current, simulation, standard test conditions

1 | INTRODUCTION

The ~25 years of service life (with ~0.7%/year degradation rate after first year) is a critical assumption in the calculation of levelized cost of energy (LCOE) for most of the photovoltaic (PV) power plants. Moreover, the annual warranted maximum degradation rates post first year are likely to further go down to 0.5%/year in near future.¹ As linear power performance warranties on modules have become commonplace in the PV industry, the power plants are scanned at regular intervals to identify underperforming PV modules for replacement. Considering the large size of utility-scale power plants, high-throughput techniques such as drone-based thermography are often used to identify faulty/underperforming modules. This technique has been successful in identifying modules that exhibit degradation modes that result in thermal signatures—such as hot-spots, cell cracks resulting in disconnected cell areas, open strings, and bypass diode failures. However, modules with degradation modes that do not result in particularly strong thermal signatures such as corrosion, light-induced degradation (LID), and potential-induced degradation (PID) are likely to be missed by this technique. Moreover, replacement clauses often require the current-voltage (I - V) measurements to be done on the PV modules. Sending large number modules from (often remotely located) power plants to test labs for accurate flash I - V measurements at Standard Test Conditions (STC) is often cost-prohibitive. This has resulted in the development of mobile test labs that can be driven to the location of PV plants for flash I - V measurements at STC. Although this approach saves the transportation cost of PV modules and avoids any damage, they may suffer during transportation; it still requires the modules to be unmounted from their structures for the measurement. Removal of the modules from the structures, handling, and reinstallation are labor intensive and can increase the chances of microcrack generation in solar cells. Due to these issues, measuring the I - V curves of modules in the field using portable I - V curve tracers is often a preferred option in several applications. The field-measured I - V curves need to be corrected to STC in order to estimate degradation rates. The International Electrotechnical Commission (IEC)² standard IEC 60891:2009 contains three procedures (called as Procedures 1, 2, and 3, respectively) for STC correction of I - V curves measured under non-STC. Procedures 1 and 2 require I - V curves measured under following conditions: (i) fixed temperature and at least three different irradiances and (ii) fixed irradiance and at least three different temperatures. Although these conditions can be achieved in a well-controlled laboratory setup, it is often difficult to achieve them in the field due to uncontrolled environmental variables. Calibrated meshes are often required to control the irradiance incident on the modules in the field, and even if instrumentation can be developed to achieve reasonably controlled conditions in the field, it would significantly increase the time required to perform I - V measurement per module. High throughput of I - V measurements is critical in the large-scale field studies such as the All India Surveys of PV Module Reliability^{3–6} and field inspections of multi-MW plants performed by diagnostics companies. Therefore, several techniques have been developed for

STC correction of field-measured I - V curves that require measurement of only one I - V curve in the field without controlling any environmental variables. Following are some of the examples of such STC correction procedures: “Modified IEC 60891-Procedure 1”,^{7,8} “Standard Irradiance and Desired Temperature” (SIDT) procedure,⁹ a procedure proposed by Anderson,¹⁰ and Voltage-Dependent Temperature Coefficient (VDTC) procedure proposed recently by Hishikawa et al.^{11,12} The IEC 60891 Procedures 1, 2, and 3, Modified IEC 60891 Procedure 1, and VDTC procedure perform STC correction of every point on the I - V curve measured at non-STC. These will be called “entire curve correction procedures” in this paper. On the other hand, SIDT and Anderson procedures perform STC correction of only key points on the I - V curve such as the short-circuit, open-circuit, and maximum power points. These will be called “point correction procedures.”

Through simulation and experimental studies, this paper investigates the accuracy in STC correction of P_{\max} , V_{oc} , FF , and I_{sc} as a function of module temperature and irradiance during I - V measurements. In addition, other factors such as measurement requirements, applicability for field studies, and dependence on temperature coefficients for various correction procedures are also discussed. Following six types of STC correction procedures are considered in this paper: IEC 60891-Procedures 1 and 2, Modified IEC 60891-Procedure 1, SIDT procedure, Anderson procedure, and VDTC procedure. IEC 60891-Procedure 3 was not included in this study, as unlike all other procedures mentioned in this paper, it is not a physics-based procedure, and also, it is rarely reported in the literature. This Procedure 3 requires at least two measured I - V curves for STC correction, and the range of correction depends on measured irradiance, temperature, and number of I - V curves. An experimental setup was developed for I - V measurements on SPIRE 5600SLP BLUE at different temperatures and irradiances. Three modules from two large-scale module manufacturers each (a total of six modules) were selected for experiments.

Simulation of I - V data was necessary due to limitations on the range of irradiance and temperature values that could be obtained in the experimental setup. For example, the accuracy of STC correction procedures for irradiance between 200 and 1300 W/m² is of interest; however, the equipment could only generate a maximum irradiance of 1100 W/m². Several simulation models based on the five-parameter single-diode equation were surveyed to generate I - V curves of modules under consideration from the I - V curve at STC. Out of these models, the model that gave the least error in the maximum power temperature coefficient (γ) of the module, when compared with the datasheet value of γ , was selected for generation of I - V curves of modules at different temperatures and irradiances.

The average percentage errors as a function of temperature and irradiance of measurement for six STC correction procedures for different performance parameters like maximum power (P_{\max}), open-circuit voltage (V_{oc}), short-circuit current (I_{sc}), and fill factor (FF) are calculated for experimental and simulation studies. Based on these and the measurement requirements, recommendations for the preferred STC correction procedure for field applications are provided.

2 | STC CORRECTION PROCEDURES

2.1 | IEC 60891-Procedure 1

Equations 1 and 2 are used in the correction of I - V curve using IEC² 60891-Procedure 1::

$$I_2 = I_1 + I_{sc} \left(\frac{G_2}{G_1} - 1 \right) + \alpha(T_2 - T_1), \quad (1)$$

$$V_2 = V_1 - R_s(I_2 - I_1) - (K I_2 - \beta)(T_2 - T_1). \quad (2)$$

where I_1 and V_1 are current and voltage coordinates of the measured I - V curve; I_2 and V_2 are coordinates of the corresponding points on the STC corrected I - V curve; G_1 is the irradiance measured with the reference device; G_2 is the irradiance at the standard or other desired irradiance (1000 W/m²); T_1 is the temperature of the test specimen; T_2 is the standard or other desired temperature (25°C); I_{sc} is the measured short-circuit current of the test specimen at G_1 and T_1 ; α and β are temperature coefficients of short-circuit current (A/°C) and open-circuit voltage (V/°C) of the test specimen, respectively; R_s is the internal series resistance of the test specimen; and K is the curve correction factor.

The recommended irradiance range for usage of this correction procedure is 800–1200 W/m². To estimate R_s , it is necessary to measure I - V curves at a fixed temperature and at least three different irradiances. On the other hand, to estimate K , it is necessary to measure I - V curves at a fixed irradiance and at least three different temperatures. As mentioned earlier, these criteria are difficult to achieve in the field unless calibrated meshes and equipment to control the module temperature are used. Brief description of IEC 60891-Procedure 2,² Modified IEC 60891-Procedure 1,^{7,8} SIDT procedure,⁹ and Anderson procedure¹⁰ are described Data S1, and Equations (S1) to (S13) are used in those procedures.

2.2 | VDTC procedure

This is an entire curve correction procedure and developed by Hishikawa et al. at AIST Japan in 2019,¹² and it requires only one I - V curve to perform the correction. However, it operates in two steps like the SIDT procedure. One point to note regarding this procedure is that it does not use open-circuit voltage or maximum power temperature coefficients (β , γ) from the module datasheet. Instead, it uses a coefficient called VDTC that can be calculated from the measured I - V curve itself.^{11,12} Unlike other temperature coefficients, VDTC is not constant, and it needs to be calculated for every coordinate on the measured I - V curve. The other parameter used in this correction procedure is series resistance (R_s), which can also be calculated from the single measured I - V curve, unlike the R_s parameter in IEC-60891 Procedures 1 and 2, which requires multiple I - V curves. Equations 3 to 6 are used in the correction of I - V curve using the VDTC procedure.

Step 1. Irradiance correction

$$I_{ICR} = I_1 + I_{sc} \left(\frac{G_2}{G_1} - 1 \right), \quad (3)$$

$$V_{ICR} = V_1 - R_s(I_{ICR} - I_1). \quad (4)$$

Step 2. Temperature correction

$$I_2 = I_{ICR} + \alpha_{rel} I_{sc_ICR}(T_2 - T_1), \quad (5)$$

$$V_2 = V_{ICR} + \frac{1}{T_1} \left(V_{ICR} - \left(\frac{N_{cell} \eta E_g}{q} \right) \right) (T_2 - T_1). \quad (6)$$

where I_{ICR} and V_{ICR} are irradiance-corrected current and voltage coordinates; η is the ideality factor of single-diode model (SDM) of PV module; E_g is the band gap of semiconductor; N_{cell} is the number of cells in the module; q is the charge of an electron; and $\frac{1}{T_1} \left(V_{ICR} - \left(\frac{N_{cell} \eta E_g}{q} \right) \right)$ is the VDTC.

The value of ηE_g for c-Si technology modules can be considered as 1.232.¹² This procedure was developed based on SDM of a PV module. Therefore, one should be careful while applying this procedure to modules with I - V curves that cannot be described adequately using SDM. Table 1 summarizes the comparison of all STC correction procedures used in this study.

3 | EXPERIMENTAL STUDY

The experimental setup and methodologies used for obtaining the I - V data of the modules at specified irradiance and temperature values with a fixed resolution in voltage (0.01 V) is described in this section. In order to experimentally estimate the accuracy of the six STC correction procedures, I - V curves of six c-Si modules (three each from two tier-1, large-scale manufacturers¹³) were measured at different temperatures and irradiances. The experimental plan included measurement of I - V curves at 10 different temperatures (25°C to 70°C with a step of 5°C) and nine different irradiances (200 to 1100 W/m², with a step of 100 W/m² [except 300 W/m², due to experimental resource constraints]).

3.1 | Experimental setup and procedure

An environmental chamber (temperature range: −40°C to 100°C) was used to heat the PV modules, and a module solar simulator (Make: SPIRE, Model: 5600SLP BLUE, Class A⁺A⁺A⁺, Flasher) was used to measure the module at nine different irradiance levels with three irradiance levels in a single flash ((1100, 1000, 900); (800, 700, 600); and (500, 400, 200)) as the module cooled down to ambient temperature of 25°C in the room. The module backsheet temperature was measured using a single infrared (IR) sensor that is integrated with the solar simulator. Figure 1 shows the

TABLE 1 Comparison summary of all 6 STC correction procedures considered in this study

STC correction procedure	Type of correction	Number of minimum curves required at various controlled conditions	Required temperature coefficients	Relative level of complexity associated with required hardware and measurement
IEC 60891-Procedure 1	Curve	5	α, β	Very high
IEC 60891-Procedure 2	Curve	5	α, β	Very high
Modified IEC 60891-Procedure 1	Curve	1	α, β	Low
SIDT	Point	1	α, β, γ	Low
Anderson	Point	1	α, β, γ	Low
VDTC	Curve	1	α	Low

Abbreviations: SIDT, Standard Irradiance and Desired Temperature; STC, Standard Test Condition; VDTC, Voltage-Dependent Temperature Coefficient.

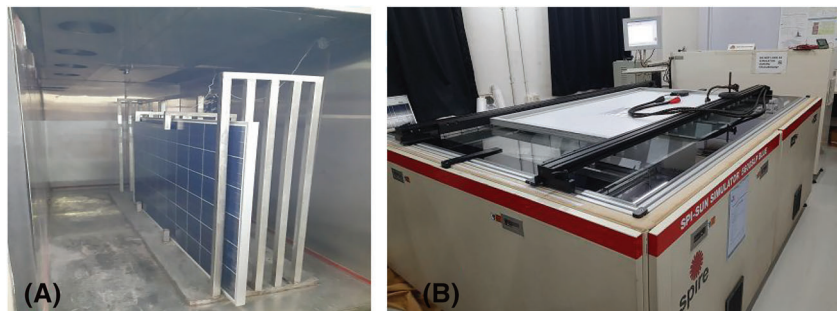


FIGURE 1 (A) Environmental chamber to heat the module and (B) solar simulator (Flasher) [Colour figure can be viewed at wileyonlinelibrary.com]

environmental chamber used for heating the modules and the solar simulator to measure the I - V of the modules at different conditions. As the solar simulator could measure I - V at a maximum of three different irradiances in a single flash, the process of heating the module and flashing it as it cooled down was repeated three times per module so that the data at nine different irradiances could be obtained. Forced air circulation in the lab was turned off to reduce the spatial nonuniformity of temperature while the module was being flashed.

3.2 | ECT determination

During the first round of measurement, the solar simulator was manually triggered to take measurements at (1100, 1000, 900) W/m^2 in a single flash once desired temperature values were reached. Similar process was repeated during the next two rounds of measurements for different sets of irradiance values. Because this process involved a manual trigger and capacitor discharge time of SPIRE Simulator, it was noticed that the backsheet temperature at which I - V was measured was slightly different than the planned temperature (Table 2). Also, in such experimental setup, the temperature of cells and that of the backsheet would be different, and this difference could be varying as a function of time. Moreover, there can be spatial nonuniformity in the temperature. In order to address these issues, the concept of equivalent cell temperature (ECT) described in IEC 60904-5:2011 was used.¹⁴

According to the IEC 60904-5:2011, the “Equivalent Cell Temperature (ECT) is the average temperature at the electronic junctions

of the device (cells, modules, arrays of one type of module) which equates to the current operating temperature if the entire device were operating uniformly at this junction temperature.” This standard applies to all the linear devices (as defined by IEC¹⁵ 60904-10:2020) with logarithmic V_{oc} dependence on irradiance irrespective of technology. The principle to find the ECT is based on the assumption of linear relationship between the open-circuit voltage (V_{oc}) of a solar cell or a module or an array and its cell temperature.¹⁴ If the open-circuit voltage (V_{oc}) of test device is known together with open-circuit voltage temperature coefficient (β), then the ECT can be determined by Equations 7 to 9.

$$V_{oc1} = V_{oc2} + V_{oc2} \left[\beta(T_1 - T_2) + a' \times \ln\left(\frac{G_1}{G_2}\right) \right], \quad (7)$$

$$ECT = T_1 = T_2 + \frac{1}{\beta} \left[\frac{V_{oc1}}{V_{oc2}} - 1 - a' \times \ln\left(\frac{G_1}{G_2}\right) \right]. \quad (8)$$

where V_{oc2} is the open-circuit voltage of test specimen at an irradiance G_2 and temperature T_2 (typically assumed to be STC, i.e., 1000 W/m^2 and 25°C, respectively); V_{oc1} is the open-circuit voltage of test specimen at an irradiance G_1 and temperature T_1 (ECT); and a' is the thermal diode voltage that can be determined from the V_{oc} measurements at a fixed temperature and varying the irradiance values. The expression for a' is given by the following equation.

$$a' = \frac{V_{oc4} - V_{oc3}}{V_{oc3} \times \ln\left(\frac{G_4}{G_3}\right)}. \quad (9)$$

TABLE 2 The values of equivalent cell temperatures (ECTs) for one of the photovoltaic (PV) modules along with actual measured backsheet temperatures and planned values of temperature to measure *I*-*V*

Planned temperature	Temperature (°C)									
	30	35	40	45	50	55	60	65	70	
Actual measured backsheet temperature	30.53	34.98	40.28	45.72	50.72	55.43	60.12	66.37	71.23	
ECT (at 200 W/m ²)	30.17	35.75	40.14	45.95	51.74	55.91	60.39	65.23	69.69	
ECT (at 400 W/m ²)	30.09	35.53	39.76	45.39	51.07	55.12	59.46	64.17	68.43	
ECT (at 500 W/m ²)	30.16	35.47	39.60	45.30	50.84	54.87	59.10	63.80	67.99	
Actual measured backsheet temperature	30.46	35.07	40.03	45.60	50.21	55.77	60.45	65.17	71.10	
ECT (at 600 W/m ²)	30.09	35.65	40.40	45.76	49.79	54.95	59.37	63.56	68.58	
ECT (at 700 W/m ²)	30.10	35.61	40.29	45.63	49.68	54.72	59.16	63.27	68.32	
ECT (at 800 W/m ²)	30.03	35.48	40.26	45.52	49.55	54.61	59.00	63.05	68.11	
Actual measured backsheet temperature	30.35	35.34	40.64	45.63	50.66	55.92	60.52	65.63	69.89	
ECT (at 900 W/m ²)	30.09	35.81	40.94	45.59	50.15	54.33	58.76	62.65	66.20	
ECT (at 1000 W/m ²)	30.05	35.71	40.89	45.53	49.97	54.18	58.56	62.45	66.05	
ECT (at 1100 W/m ²)	29.97	35.73	40.78	45.38	49.87	54.12	58.46	62.34	65.87	

One of the irradiances between G_3 and G_4 can be considered equal to G_2 which is 1000 W/m^2 . In the experiment, G_4 was considered to be 800 W/m^2 , and for both the irradiance conditions, the temperature was 25°C . The temperatures at which it was planned to measure the *I*-*V* curves, actual measured backsheet temperatures, and the calculated ECT values using IEC 60904-5 for one of the modules are given in Table 2.

3.3 | Regeneration of *I*-*V* curves at planned temperatures

It can be seen from the columns in Table 2 that the ECT values in any given column at various irradiances are close to each other, but they are not exactly the same. Similar observation was noted for all six modules. In order to provide a uniform basis for assessing the accuracy of various STC correction procedures, it was important to have the *I*-*V* curves at various irradiances and exactly same temperatures (“planned temperatures”). Therefore, for each irradiance value in Table 2, the *I*-*V* curve was corrected to “planned temperature” using the IEC 60891-Procedure 2. Because the difference between the ECT values in each column and planned temperatures is small ($<5^\circ\text{C}$), the errors introduced in this transformation are negligible. Also, as will be shown later, the errors introduced in STC correction using IEC 60891-Procedure 2 are anyway small even while correcting for STC from fairly high temperatures.

3.4 | Curve fitting and data interpolation

The measured and regenerated *I*-*V* curves of all the modules have different numbers of data points. Also, these data points are not equally spaced apart in terms of voltage. In order to get equally spaced *I*-*V* data points with a voltage resolution of 0.01 V, the *I*-*V*

curve was interpolated using SDM. Figure S1 shows the comparison of regenerated and curve-fitted *I*-*V* curves of a PV module at 70°C .

4 | SIMULATION STUDY

In order to complement the experimental data, a simulation model was also developed for acquiring the *I*-*V* data of PV modules at specified irradiance and temperature values. The simulation model was useful in extrapolating the data to 1200 W/m^2 and beyond as the experimental setup was limited to 1100 W/m^2 . The simulation model was also useful to interpolate the data at intermediate values of irradiance and temperatures where the experimental data were not available. The simulation model was selected after a comparative accuracy assessment of eight different models from the literature using the methodology described below in Section 4.1. Each simulation model is defined by five sets of translation equations, one for each of the five SDM parameters (photocurrent [I_{ph}], reverse saturation current [I_{sat}], ideality factor [η], series resistance (R_s), and shunt resistance [R_{sh}]). A translation equation transforms each SDM parameter value at STC to a specified irradiance and temperature.

4.1 | Selection of best simulation model for *I*-*V* generation of a PV module

The PV module was modeled with five-parameter SDM. Figure S2 shows the SDM of a PV module, and the current equation of PV module is given by Equation 10.¹⁶ SDM parameters (I_{ph} , I_{sat} , η , R_s , and R_{sh}) of all PV modules at STC were extracted using experimental data (V_{oc} , I_{sc} , P_{max} , V_{mp} , I_{mp} , and FF) measured at STC. This can also be accomplished by using the same (nominal) information given in module datasheets.¹⁷

$$I = I_{ph} - I_{sat} \left(\exp \left(\frac{V + IR_s}{\eta N_{cell} V_t} \right) - 1 \right) - \frac{V + IR_s}{R_{sh}}. \quad (10)$$

where N_{cell} is the number of cells in the PV module and V_t is the thermal voltage.

In this exercise, eight different simulation models^{16,18} were considered. Each simulation model had a translation equation for transforming each SDM parameter at STC to specified value of irradiance (G) and temperature (T). These models differed from each other in at least one translational equation. The goal was to identify a simulation model that would be successful in predicting the I - V curves of PV modules at any specified G and T with highest accuracy. For this, I - V data for each module were generated using all eight simulation models at 1000 W/m² and at various temperatures (25°C to 70°C with a step of 5°C). Then, the temperature coefficient of maximum power (γ) was calculated from the simulated data for each model, and the relative percentage error in γ was calculated by comparing those values with the ones given in the module

datasheets (the experimentally obtained maximum power temperature coefficients are also very similar to datasheet values with error less than 3%). The reason for choosing γ as the metric for accuracy of a simulation model was that all other parameters given in the datasheet (such as other temperature coefficients α , β) were used as input in at least one of the simulation models, while γ was not used by any of the simulation models as an input. Also, another advantage of choosing this metric is that one can compare the accuracy of various simulation models just based on the information given in the module datasheets—without having to perform any additional experimental characterization. Figure 2 shows the comparison of relative percentage errors in γ for all modules and all simulation models. It can be seen that the Simulation Model 2 consistently produces the least error for all the modules. Therefore, it was chosen for generating the I - V data for modules at various temperatures and irradiances.

4.2 | Brief description and comparison of all tested simulation models

The set of equations for all the SDM parameters at any desired G and T can be expressed in terms of their values extracted at STC (Equations 11 to 28). The equations for all the SDM parameters used in Simulation Model 2 in comparison with all other tested models were tabulated in Table 3.

- Series resistance ($R_s(G, T)$):

$$R_s(G, T) = R_s(STC), \quad (11)$$

$$R_s(G, T) = \left(\frac{T}{T(STC)} \right) \left[1 - 0.217 \ln \left(\frac{G}{G(STC)} \right) \right] R_s(STC), \quad (12)$$

$$R_s(G, T) = R_s(STC) \left(\frac{\frac{G(STC)}{G} \left(\frac{T(STC)}{T} \right)^{\gamma}}{\left(1 + \beta \ln \left(\frac{G(STC)}{G} \right) \right) \left(1 + \frac{\alpha(T - T(STC))}{I_{mp}(G, T)} \right)} \right). \quad (13)$$

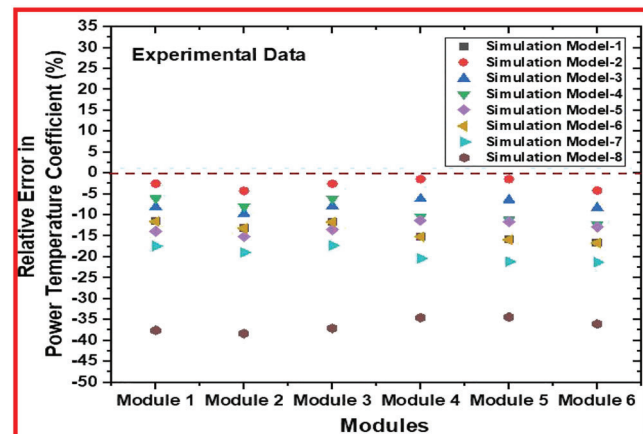


FIGURE 2 Comparison of percentage error in maximum power temperature coefficient (γ) for all the eight tested simulation models for each of the six modules using experimental parameters [Colour figure can be viewed at wileyonlinelibrary.com]

Simulation model	Equation used for each SDM parameter				
	$R_s(G, T)$	$R_{sh}(G, T)$	$\eta(G, T)$	$I_{sat}(G, T)$	$I_{ph}(G, T)$
1	11	14	15	17	19
2	12	14	15	18	20
3	11	14	15	18	20
4	12	14	15	17	20
5	13	14	15	18	20
6	11	14	15	17	20
7	13	14	15	17	20
8	13	14	16	18	20

Abbreviation: SDM, single-diode model.

TABLE 3 Comparison of all eight simulation models tested in this study through SDM parameters

- Shunt resistance ($R_{sh}(G, T)$):

$$R_{sh}(G, T) = \left(\frac{G(STC)}{G} \right) R_{sh}(STC). \quad (14)$$

- Open-circuit voltage ($V_{oc}(G, T)$):

$$V_{oc}(G, T) = \left(\frac{V_{oc}(STC)}{1 + b \times \ln\left(\frac{G(STC)}{G}\right)} \right) \left(\frac{T(STC)}{T} \right)^y, \quad (22)$$

- Ideality factor ($\eta(G, T)$):

$$\eta(G, T) = \eta(STC), \quad (15)$$

$$b = \frac{\left(\left(\frac{V_{oc}(STC)}{V_{oc}(G)} \right) - 1 \right)}{\ln\left(\frac{G(STC)}{G}\right)}, \quad (23)$$

$$\eta(G, T) = \left(\frac{V_{mp}(G, T) + I_{mp}(G, T)R_s(G, T)}{V_{mp}(T)N_{cell}} \right) \left(\frac{1}{\ln\left(I_{ph}(G, T) - I_{mp}(G, T)\left(1 + \frac{R_s(G, T)}{R_{sh}(G, T)}\right) - \frac{V_{mp}(G, T)}{R_{sh}(G, T)}\right) - \ln\left(I_{ph}(G, T) - \frac{V_{oc}(G, T)}{R_{sh}(G, T)}\right)} \right). \quad (16)$$

- Reverse saturation current ($I_{sat}(G, T)$):

$$V_{oc}(G) = \ln\left(\frac{I_{ph}(G)R_{sh}(G) - V_{oc}(G)}{I_{sat}(STC)R_{sh}(G)}\right) \eta(STC)N_{cell}V_t, \quad (24)$$

$$I_{sat}(G, T) = I_{sat}(STC) \left(\frac{T}{T(STC)} \right)^3 \exp\left(\left(\frac{qE_g(T)}{\eta(G, T)N_{cell}K_B} \right) \left(\frac{1}{T(STC)} - \frac{1}{T} \right) \right), \quad (17)$$

$$y = \frac{\ln\left(\frac{V_{oc}(STC)}{V_{oc}(T)}\right)}{\ln\left(\frac{T}{T(STC)}\right)}, \quad (25)$$

$$I_{sat}(G, T) = \frac{\left(1 + \frac{R_s(G, T)}{R_{sh}(G, T)}\right)I_{sc}(G, T) - \frac{V_{oc}(G, T)}{R_{sh}(G, T)}}{\exp\left(\frac{V_{oc}(G, T)}{\eta(G, T)N_{cell}V_t}\right) - \exp\left(\frac{I_{sc}(G, T)R_s(G, T)}{\eta(G, T)N_{cell}V_t}\right)}. \quad (18)$$

where

$$V_{oc}(T) = V_{oc}(STC) + \beta(T - T(STC)). \quad (26)$$

- Photocurrent ($I_{ph}(G, T)$):

$$I_{ph}(G, T) = I_{sc}(G, T) \left(1 + \frac{R_s(G, T)}{R_{sh}(G, T)} \right), \quad (19)$$

- Maximum power voltage ($V_{mp}(G, T)$):

$$V_{mp}(G, T) = \left(\frac{V_{mp}(STC)}{1 + b \times \ln\left(\frac{G(STC)}{G}\right)} \right) \left(\frac{T(STC)}{T} \right)^y. \quad (27)$$

$$I_{ph}(G, T) = \frac{I_{sc}(G, T) \left(1 + \frac{R_s(G, T)}{R_{sh}(G, T)} \right) \left(\exp\left(\frac{V_{oc}(G, T)}{\eta(G, T)N_{cell}V_t}\right) - 1 \right) - \frac{V_{oc}(G, T)}{R_{sh}(G, T)} \left(1 - \exp\left(\frac{I_{sc}(G, T)R_s(G, T)}{\eta(G, T)N_{cell}V_t}\right) \right)}{\exp\left(\frac{V_{oc}(G, T)}{\eta(G, T)N_{cell}V_t}\right) - \exp\left(\frac{I_{sc}(G, T)R_s(G, T)}{\eta(G, T)N_{cell}V_t}\right)}. \quad (20)$$

- Short-circuit current ($I_{sc}(G, T)$):

$$I_{sc}(G, T) = \left(\frac{G}{G(STC)} \right) [I_{sc}(STC) + \alpha(T - T(STC))]. \quad (21)$$

- Maximum power current ($I_{mp}(G, T)$):

$$I_{mp}(G, T) = \left(\frac{G}{G(STC)} \right) [I_{mp}(STC) + \alpha(T - T(STC))]. \quad (28)$$

4.3 | Comparison of module I–V generated through simulation with the experiment

Using the SDM parameter equations from “Model 2” and all other simulation models, the *I*–*V* curves of all six PV modules were generated at various temperature and irradiance conditions. To find the accuracy of all simulation models, the generated *I*–*V* curves were compared with the experimentally measured *I*–*V* curves for all the modules. Figure 3 shows the comparison of simulated (Model 2) and experimentally measured (regenerated using ECT values) *I*–*V* characteristics with reference to a parameter called average root mean square error (ARMSE). In order to calculate root mean square error (RMSE), RMSE is calculated point-by-point between the simulated and experimental *I*–*V* curves of the same module, under the same conditions. ARMSE is then calculated by averaging the RMSE for all the six modules at each condition of temperature and irradiance. The ARMSE values averaged across all conditions for all the eight tested simulation models, and their values are tabulated in Table 4. The lowest value of averaged ARMSE is achieved for Simulation Model 2 (0.13), and this gave more confidence to the methodology of using percentage error in γ while choosing simulation model.

The generated *I*–*V* curves through Simulation Model 2 were found to be in close agreement with the experimental *I*–*V* curves (Figure 4). The observed values of higher errors at very low irradiance

and high temperature conditions might be due to the change in temperature coefficient value with irradiance (observed in experimental data; Figure S3),^{19–22} which we considered as constant in simulation. The percentage errors in key performance parameters maximum power (P_{max}) and open-circuit voltage (V_{oc}) were observed to be within $\pm 1\%$ and (+1.3%, -0.35%), respectively, for the simulation and experimental results. Highest percentage error in V_{oc} (+1.3%) was observed under the conditions of lowest irradiance: 200 W/m² and at highest temperature: 70°C. It should be noted that such a combination of irradiance and temperature is rarely encountered in the field. One can also observe the higher ARMSE in Figure 3 under the same conditions.

5 | RESULTS AND DISCUSSIONS

Experimentally measured *I*–*V* curves of all the six modules (regenerated after using ECT values) and the corresponding *I*–*V* curves generated by Simulation Model 2 for each module were given as inputs to all the six STC correction procedures. The percentage errors in the STC corrected parameters for various irradiance and temperature *I*–*V* curves relative to experimentally measured parameters at STC were calculated for all the six modules. Percentage errors in each performance parameter (P_{max} , V_{oc} , I_{sc} , and FF) were averaged across

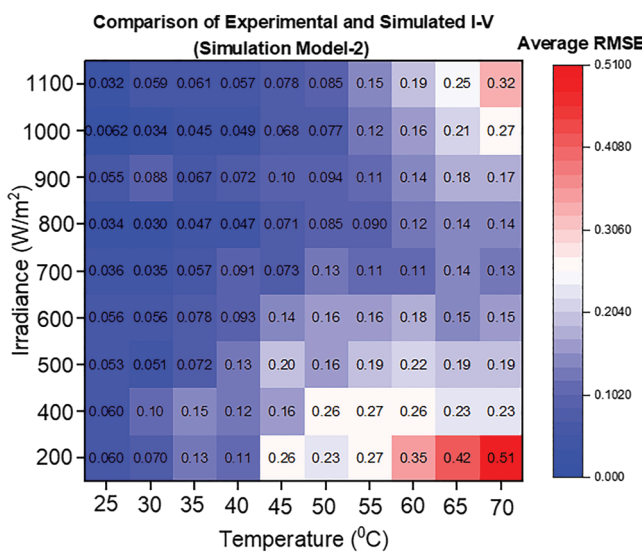


FIGURE 3 Heatmap of average root mean square error (ARMSE) for all the *I*–*V* curves between experimental (regenerated using equivalent cell temperature [ECT] values) and simulated (Model 2) [Colour figure can be viewed at wileyonlinelibrary.com]

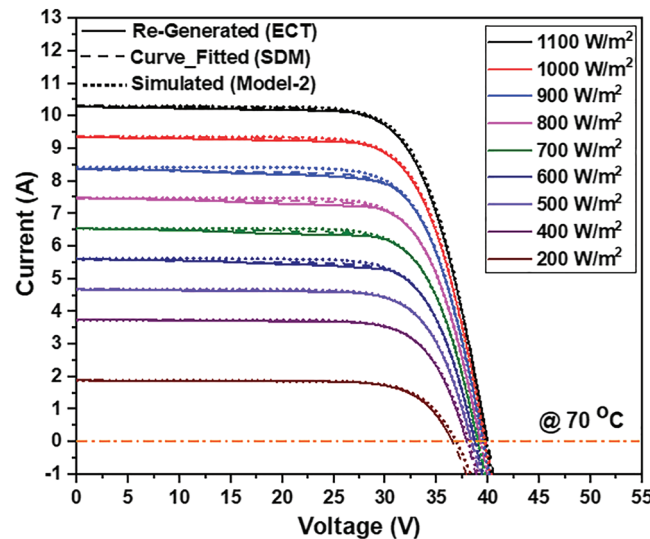


FIGURE 4 Comparison of experimental (regenerated using equivalent cell temperature [ECT] values), curve-fitted (using single-diode model [SDM]), and simulated (Model 2) *I*–*V* curves of a photovoltaic (PV) module at 70°C [Colour figure can be viewed at wileyonlinelibrary.com]

Simulation model (SM)	1	2	3	4	5	6	7	8
Averaged ARMSE	0.25	0.13	0.25	0.16	1.36	0.24	1.37	1.36

Abbreviation: ARMSE, average root mean square error.

TABLE 4 Comparison of averaged ARMSE of all eight simulation models tested in this study

six modules, and contour plots were generated to show the dependence of errors on irradiance and temperature during the measurement.

5.1 | Comparison of STC corrected *I*-*V* curves for different procedures

IEC 60891-Procedures 1 and 2, Modified IEC 60891-Procedure 1, and VDTC procedure are entire curve correction procedures. Figures 5 to 8 show the STC corrected *I*-*V* curves for the experimental and simulated input data at 70°C for one of the modules by all the four curve correction procedures. In case of IEC 60891-Procedure 1, the differences can be observed from the maximum power point to open-circuit region of STC corrected *I*-*V* curves for experimental and simulated input data (Figure 5A,B). This is due to the differences in

experimental and simulated input data as the irradiance is decreasing, and IEC 60891-Procedure 1 does not use irradiance correction factor for V_{oc} unlike IEC 60891-Procedure 2.

Figure S4 shows the heatmap of ARMSE of six modules between the *I*-*V* curves that were measured at STC and the *I*-*V* curves that were measured at other conditions but corrected to STC using the above four procedures. It can be seen that the VDTC procedure is producing lower ARMSE values compared with the other three procedures.

5.2 | Irradiance and temperature dependence of errors in key performance parameters

The expression for the percentage error in any performance parameter is given by Equation 29:

FIGURE 5 Standard Test Condition (STC) translated *I*-*V* curves using IEC 60891-Procedure 1 (A) for experimental and (B) for simulated input data at 70°C and at all the tested irradiance conditions [Colour figure can be viewed at wileyonlinelibrary.com]

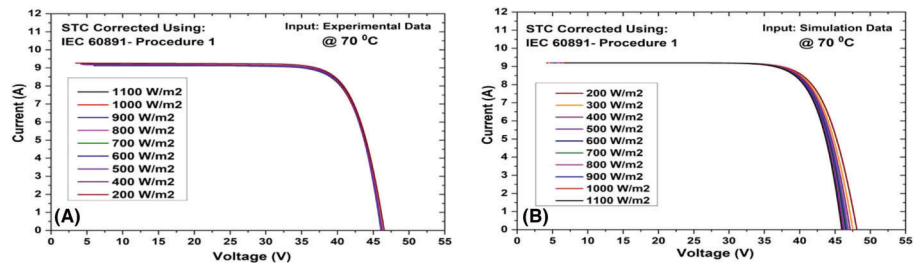


FIGURE 6 Standard Test Condition (STC) translated *I*-*V* curves using IEC 60891-Procedure 2 (A) for experimental and (B) for simulated input data at 70°C and at all the tested irradiance conditions [Colour figure can be viewed at wileyonlinelibrary.com]

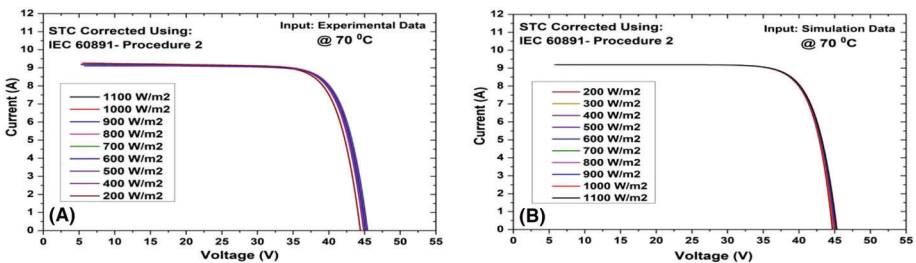


FIGURE 7 Standard Test Condition (STC) translated *I*-*V* curves using Modified IEC 60891-Procedure 1 (A) for experimental and (B) for simulated input data at 70°C and at all the tested irradiance conditions [Colour figure can be viewed at wileyonlinelibrary.com]

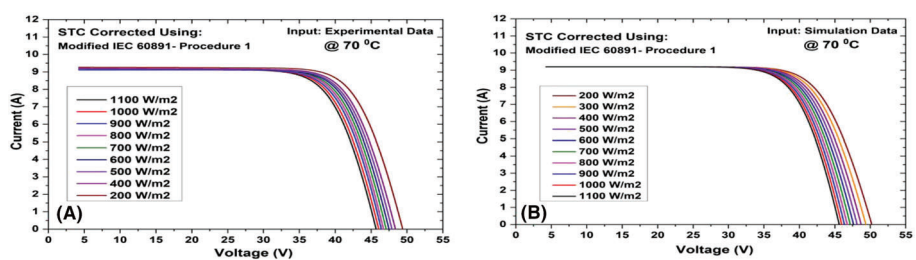
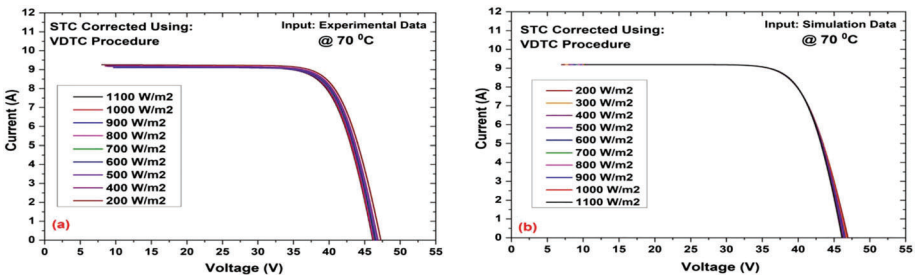


FIGURE 8 Standard Test Condition (STC) translated *I*-*V* curves using Voltage-Dependent Temperature Coefficient (VDTC) procedure (A) for experimental and (B) for simulated input data at 70°C and at all the tested irradiance conditions [Colour figure can be viewed at wileyonlinelibrary.com]



$$\text{Percentage Error (\%)} = \left(\frac{\text{Value Obtained After Corrected to STC} - \text{Actual Value at STC}}{\text{Actual Value at STC}} \right) * 100. \quad (29)$$

The average (from six modules) percentage errors in P_{\max} (Figures 9 to 14), V_{oc} (Figures S5 to S10), I_{sc} (Figure S11), and FF (Figures S12 to S17) produced by all the six STC correction procedures for experimental and simulated input I-V curves were compared.

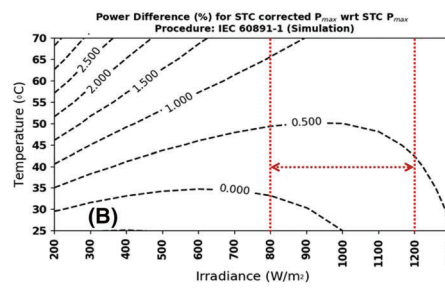
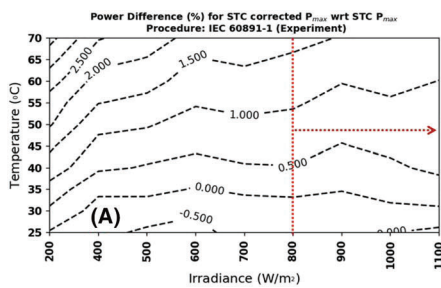


FIGURE 9 Average percentage error in P_{\max} produced by IEC 60891-Procedure 1 for (A) experimental and (B) simulated input data [Colour figure can be viewed at wileyonlinelibrary.com]

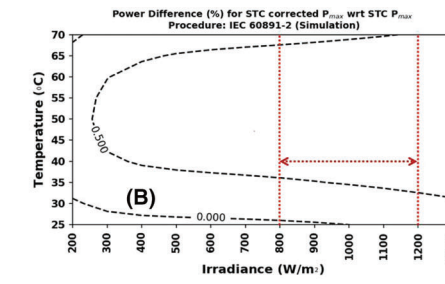
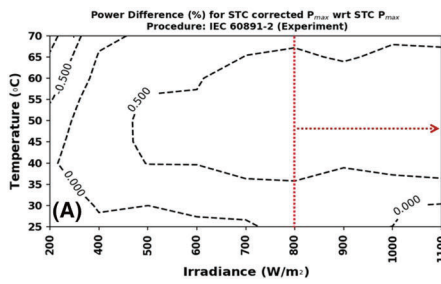


FIGURE 10 Average percentage error in P_{\max} produced by IEC 60891-Procedure 2 for (A) experimental and (B) simulated input data [Colour figure can be viewed at wileyonlinelibrary.com]

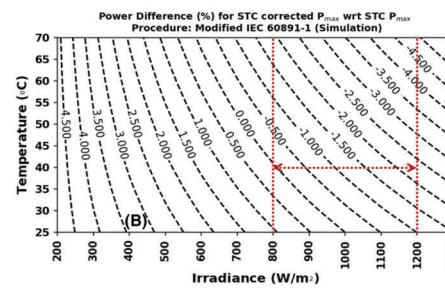
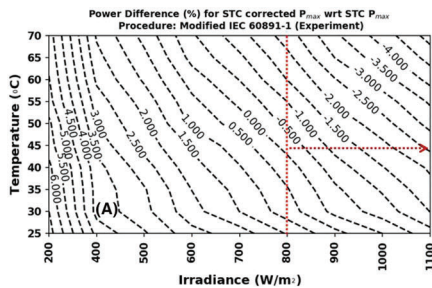


FIGURE 11 Average percentage error in P_{\max} produced by modified IEC 60891-Procedure 1 for (A) experimental and (B) simulated input data [Colour figure can be viewed at wileyonlinelibrary.com]

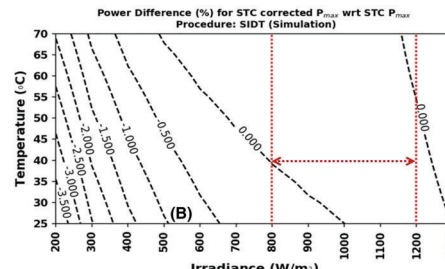
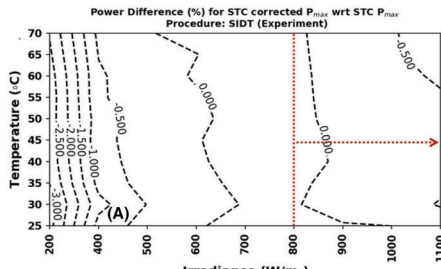


FIGURE 12 Average percentage error in P_{\max} produced by Standard Irradiance and Desired Temperature (SIDT) procedure for (A) experimental and (B) simulated input data [Colour figure can be viewed at wileyonlinelibrary.com]

FIGURE 13 Average percentage error in P_{\max} produced by Anderson procedure for (A) experimental and (B) simulated input data [Colour figure can be viewed at wileyonlinelibrary.com]

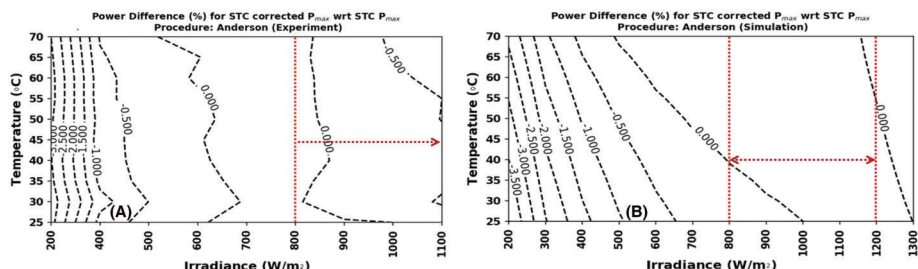


FIGURE 14 Average percentage error in P_{\max} produced by Voltage-Dependent Temperature Coefficient (VDTC) procedure for (A) experimental and (B) simulated input data [Colour figure can be viewed at wileyonlinelibrary.com]

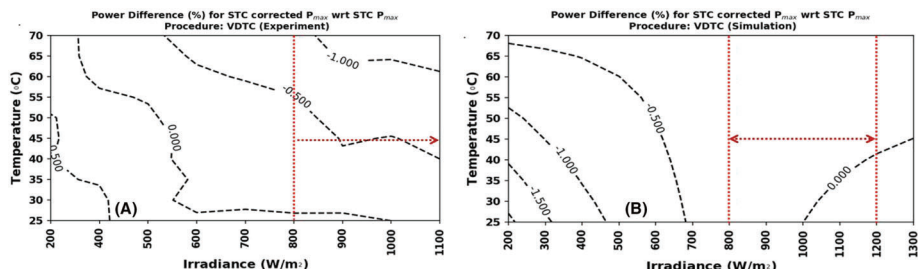


TABLE 5 Minimum and maximum average percentage error in P_{\max} produced by different STC correction procedures for experimental and simulated input data

Correction procedures	Parameter (P_{\max})			
	Experiment		Simulation	
	800–1100 (200–1100) W/m ²	800–1200 (200–1300) W/m ²	800–1200 (200–1300) W/m ²	800–1200 (200–1300) W/m ²
Minimum (%)	Maximum (%)	Minimum (%)	Maximum (%)	Minimum (%)
IEC 60891-Procedure 1	-0.34 (-0.59)	1.65 (3.67)	-0.26 (-0.51)	1.13 (3.66)
IEC 60891-Procedure 2	-0.10 (-1.17)	0.95 (0.95)	-0.06 (-0.29)	0.94 (0.99)
Modified IEC 60891-Procedure 1	-5.21 (-5.21)	1.46 (6.71)	-4.94 (-5.62)	1.06 (4.86)
SIDT	-0.80 (-3.22)	0.19 (0.19)	-0.19 (-4.01)	0.32 (0.32)
Anderson	-0.98 (-3.29)	0.19 (0.20)	-0.19 (-4.01)	0.39 (0.39)
VDTC	-1.26 (-1.26)	0.16 (0.76)	-0.42 (-2.09)	0.23 (0.34)

Abbreviations: SIDT, Standard Irradiance and Desired Temperature; STC, Standard Test Condition; VDTC, Voltage-Dependent Temperature Coefficient.

highlight the errors in the range of 800–1100 W/m² (800–1200 W/m²) for experimental (simulated) input data. The errors in the range of 800–1200 W/m² are of interest as it is the recommended measurement range in IEC 60891.²

Among the “entire curve correction procedures,” IEC 60891-Procedures 1 and 2 and VDTC were seen to produce lower errors than the Modified IEC 60891-Procedure 1 when the irradiance range was 800–1200 W/m² (Table 5). Modified IEC 60891-Procedure 1 produces higher errors as it does not use series resistance and curve correction factors in the correction. The point correction procedures: SIDT and Anderson procedures produce comparable errors in this irradiance range; however, their errors increase at lower irradiances. It should be noted that the SIDT and Anderson procedures use γ in the correction along with α and β , so these procedures are sensitive to the possible errors in all of the temperature coefficients. Compared with all procedures, the VDTC procedure produces lower error when the

entire 200–1300-W/m² irradiance range is considered. The possible reasons for the superior performance of VDTC procedure on a wide range of irradiance values are the following: (i) unlike other procedures, it uses a VDTC,¹² which is calculated for every point of the I - V curve. Note other procedures assume constant β . (ii) It uses the series resistance parameter in correction, which can be calculated from the single measured I - V curve, and it varies based on measured irradiance and temperature conditions. Note that IEC 60891-Procedures 1 and 2 use a constant R_s . The differences observed in the contour plots of average percentage errors produced by VDTC procedure (Figure 14A, B) for experimental to simulated inputs are due to variation in series resistance as a function of irradiance. The contour algorithm uses linear interpolation to generate continuous contour curve in between the data points.

Least errors in V_{oc} correction were observed in case of VDTC procedure with the percentage errors within 0% to -0.5% for the

irradiance range of 800–1200 W/m². The superior performance is attributed to the use of VDTC and series resistance for correction. The contour plots of percentage errors in V_{oc} (Figures S5 to S10) for experimental and simulated inputs are similar in shape for individual correction procedures. Modified IEC 60891-Procedure 1 predicts higher values of V_{oc} (error is positive for irradiance < 1000 W/m²), and SIDT and Anderson procedures perform similarly, but they predict lower values of V_{oc} (error is negative for irradiance < 1000 W/m²). SIDT and Anderson procedures produce more errors as the irradiance decreases, as they do not perform any correction for irradiance on V_{oc} . For IEC 60891-Procedure 1, the differences in magnitude of percentage errors were observed to be significant between experiment and simulation data as the irradiance is decreasing. The reasons for this are the following: (i) deviation in simulated I - V curves from the experimental I - V curves (especially around open-circuit region). (ii) IEC 60891-Procedure 1 does not use irradiance correction factor for V_{oc} unlike IEC 60891-Procedure 2.

The contour plot of percentage errors in I_{sc} produced by IEC 60891-Procedure 2 for simulated input is shown in Figure S11. Similar contour plots and magnitudes were observed for all other procedures for simulated and experimental data. It was found that the percentage errors in I_{sc} were negligible. Significantly lower value of temperature coefficient of current as compared with other temperature coefficients and approximate linearity of I_{sc} with irradiance is responsible for the negligible percentage errors in the corrected I_{sc} .

The FF is calculated using Equation 30

$$FF = \frac{V_{mp}I_{mp}}{V_{oc}I_{sc}}. \quad (30)$$

The contour plots of percentage errors in FF produced by individual STC correction procedures (Figures S12 to S17) for experimental and simulated inputs are similar in shape. Modified IEC 60891-Procedure 1 predicts lower values of FF than actual (error is negative for irradiance < 1000 W/m²), and SIDT and Anderson procedures perform similarly, but they predict higher values of FF (error is positive irradiance < 1000 W/m²). These errors increase in magnitude as the irradiance decreases. This is evident from Equation 30 and the fact that Modified IEC-60891 Procedure predicts higher V_{oc} while SIDT and Anderson procedures predict lower V_{oc} at irradiance < 1000 W/m². Also, errors in I_{sc} are negligible as discussed before. VDTC procedure predicts FF with reasonable accuracy (error is within –2.2 to +0.15%) and is better compared with Modified IEC 60891-Procedure, SIDT procedure, and Anderson procedure.

The estimated percentage errors in STC correction of various performance parameters are also valid for the bifacial c-Si PV modules. Bifacial PV modules made up of solar cell technologies that have improved low light response (PERC, PERL, PERT, IBC, and HJT) than conventional Al-BSF monofacial module technology. The I - V curves of bifacial modules measured either in the lab or in the field according to IEC²³ TS 60904-1-2 can be corrected to STCs using all the six STC correction procedures. For bifacial modules made up of PERC, PERL, PERT, and IBC technologies, the VDTC procedure can be directly

applied and the error calculation is also valid (tuning the value of ηE_g may still result in better correction). But for bifacial (or monofacial) modules with HJT technology, precise formulation of VDTC is required¹¹ as HJT devices are made of heterojunction of amorphous silicon and crystalline silicon rather than a homo junction of crystalline silicon.

6 | CONCLUSION

The accuracy in STC correction, simplicity of use, and applicability to field I - V measurements were compared for six different STC correction procedures through experimental and simulation studies. The curve correction procedures, IEC 60891-Procedures 1 and 2, were shown to deliver high accuracy in STC correction for most of the tested temperature and irradiance range (especially in 800–1200 W/m²). However, these procedures require multiple I - V curves at controlled temperature and irradiance. This severely limits the prospects of applying these procedures in the field for large-scale I - V measurements as they would require special equipment and sophisticated procedure for achieving the temperature and irradiance control in the field. This often results in significantly more time being spent per module, and therefore, these procedures would not be suitable for high-throughput field measurement applications. The advantages of Modified IEC 60891-Procedure 1 include it being an entire curve correction procedure and requirement of just a single I - V curve. Thus, it can be useful in field measurements due to its high throughput. However, this procedure was shown to have lower accuracy than the other curve correction procedures. Also, there is a systematic bias in the Modified IEC 60891-Procedure 1, as it predicts higher values of V_{oc} and consequently lower values of FF below 1000 W/m². SIDT and Anderson procedures also require just a single curve each and provide better accuracy than the Modified IEC 60891-Procedure 1 in the irradiance range of 800–1200 W/m². However, these are point correction procedures; therefore, they do not provide the entire I - V curve at STC. This can make the calculation of series and shunt resistance more difficult. Also, it should be noted that these procedures will be sensitive to errors in all of the temperature coefficients as they use all three temperature coefficients. Moreover, they also suffer from systematic bias and predict lower values of V_{oc} and consequently higher values of FF below 1000 W/m². It has been shown that the recently proposed VDTC procedure has several advantages over existing procedures such as it being a curve correction procedure, requirement of just a single I - V curve, and most importantly, delivering high accuracy—which is comparable with or sometimes more than IEC 60891-Procedures 1 and 2 (which require multiple I - V curves). Another advantage of this procedure is that it only uses the current temperature coefficient and therefore is not sensitive to the errors in the temperature coefficients of V_{oc} and P_{max} . However, VDTC procedure would only be applicable to c-Si PV modules whose I - V curve can be adequately described by a SDM. Provided this requirement is met, VDTC procedure is shown to be most suitable for field applications. For bifacial PV modules, once the current–voltage (I - V) curves

are measured either in indoor or in outdoor according to IEC TS 60904-1-2, the STC correction errors in different performance parameters produced by the STC correction procedures considered in this paper are still valid.

Among the existing three temperature coefficients (α , β , and γ), the uncertainty in estimation of short-circuit current temperature coefficient (α) is likely to be highest due to following reasons^{24,25}: (i) spectral irradiance mismatch with respect to reference AM1.5G spectrum of STC and (ii) mismatch in the spectral response (SR) between reference device and the device under test. Even though the absolute value of α ($\sim +0.05\%/\text{°C}$ for c-Si technology) is very small, large uncertainties in it will lead to reasonable errors in STC correction of various performance parameters. To avoid this, spectral mismatch correction should be performed by considering the variation of SR with temperature.²⁵ The effect of uncertainties in the temperature coefficients of P_{\max} , V_{oc} , and I_{sc} on the errors in STC correction of various procedures is being investigated by the authors.

In addition, through a comparative assessment of eight simulation models, a simulation model has been identified in this paper which enables accurate prediction of the I - V curve of a PV module at any temperature and irradiance. Even outside of the context of STC correction procedures, the simulation model can be used in general for accurate PV performance prediction. Moreover, the experimental setup and techniques for error correction presented in this paper would have wide applicability. For example, these experiments can be performed on any sun simulator—even on those simulators that do not have sophisticated attachments of environmental chambers for temperature control.

ACKNOWLEDGEMENTS

The authors would like to acknowledge Prof. B. M. Arora, Prof. K. L. Narasimhan, and Dr. Hemant Kumar for their inputs during the discussions. The authors would also like to thank Mr. Rambabu Sugguna, Mr. Ajeesh Alath, and Mr. Ritesh Ingle for helping during the experiments. This work was supported by NCPRE funded by the Ministry of New and Renewable Energy of the Government of India through Project No. 31/09/2015-16/PVSE-R&D dated 15 June 2016.

CONFLICT OF INTEREST

The authors confirm that there is no conflict of interest in this study.

DATA AVAILABILITY STATEMENT

Research data are not shared.

ORCID

Yogeswara Rao Golve  <https://orcid.org/0000-0002-2726-2874>

Anil Kottantharayil  <https://orcid.org/0000-0002-5208-1012>

Narendra Shiradkar  <https://orcid.org/0000-0003-2272-9954>

REFERENCES

1. ITRPV. 2020. <https://itrpv.vdma.org/documents/27094228/29066965/ITRPV02020Presentation0-0USA/0bbc457b-c90be51f-20ac-ed6c2138fe1a>
2. International Electrotechnical Commission (IEC). IEC 60891 Standard Edition 2.0, 2009-12.
3. Dubey R, Chattopadhyay S, Kuthanazhi V, et al. All-India survey of photovoltaic module degradation: 2013. Technical Report Published by the National Centre for Photovoltaic Research and Education (NCPRE), IIT Bombay and National Institute of Solar Energy (NISE); 2014.
4. Dubey R, Chattopadhyay S, Kuthanazhi V, et al. All-India survey of photovoltaic module reliability: 2014. Technical Report Published by the National Centre for Photovoltaic Research and Education (NCPRE), IIT Bombay and National Institute of Solar Energy (NISE); 2016.
5. Chattopadhyay S, Dubey R, Kuthanazhi V, et al. All-India survey of photovoltaic module reliability: 2016. Technical Report Published by the National Centre for Photovoltaic Research and Education (NCPRE), IIT Bombay and National Institute of Solar Energy (NISE); 2017.
6. Golve YR, Zachariah S, Bhaduri S, et al. All-India survey of photovoltaic module reliability: 2018. Technical Report Published by the National Centre for Photovoltaic Research and Education (NCPRE), IIT Bombay and National Institute of Solar Energy (NISE); 2019.
7. Dubey R, Chattopadhyay S, Kuthanazhi V, et al. Performance degradation in field-aged crystalline silicon PV modules in different Indian climatic conditions. 40th IEEE Photovoltaic Specialists Conference, Denver, USA; 2014:3182-3187.
8. Herrmann W, Wiesner W. Current-voltage translation procedure for PV generators in the German 1000 Roofs Programme. http://www.f09.fhkoeln.de/imperia/md/content/personen/wiesner_wolfgang/veroeffentlichungen/26_proceed.pdf
9. Singh HK, Dubey R, Zachariah S, et al. Modified STC correction procedure for assessing PV module degradation in field survey. 44th IEEE Photovoltaic Specialist Conference, Washington DC, USA; 2017: 1995-1997.
10. Anderson AJ. Photovoltaics translation equations: a new approach. Sunset Technology, January 1996, NREL/TP-411-20279.
11. Hishikawa Y, Doi T, Higa M, et al. Voltage-dependent temperature coefficient of the I - V curves of crystalline silicon photovoltaic modules. *IEEE J Photovolt.* 2018;8(1):48-53. <https://doi.org/10.1109/JPHOTOV.2017.2766529>
12. Hishikawa Y, Takenouchi T, Higa M, Yamagoe K, Ohshima H, Yoshita M. Translation of solar cell performance for irradiance and temperature from a single I - V curve without advance information of translation parameters. *IEEE J Photovolt.* 2019;9(5):1195-1201. <https://doi.org/10.1109/JPHOTOV.2019.2924388>
13. <https://review.solar/latest-tier-1-solar-panels-list-2019/>
14. International Electrotechnical Commission (IEC). IEC 60904-5: 2011 Standard.
15. International Electrotechnical Commission (IEC). IEC 60904-10: 2020 Standard.
16. Ibrahim H, Anani N. Variations of PV module parameters with irradiance and temperature. 9th International Conference on Sustainability in Energy and Buildings, Energy Procedia; 2017;134:276-285. <https://doi.org/10.1016/j.egypro.2017.09.617>
17. Dongue SB, Njomo D, Ebengai L. An improved nonlinear five-point model for photovoltaic modules. *Int J Photoenergy.* 2013;2013:1-11. <https://doi.org/10.1155/2013/680213>
18. Hejri M, Mokhtari H, Azizian MR, Söder L. An analytical-numerical approach for parameter determination of a five parameter single-diode model of photovoltaic cells and modules. *Int J Sustain Energy.* 2016;35(4):396-410. <https://doi.org/10.1080/14786451.2013.863886>
19. Cotfas DT, Cotfas PA, Machidon OM. Study of temperature coefficients for parameters of photovoltaic cells. *Int J Photoenergy.* 2018; 2018:1-12. <https://doi.org/10.1155/2018/5945602>

20. Tayyib M, Odden JO, Saetre TO. Irradiance dependent temperature coefficients for MC solar cells from Elken solar grade silicon in comparison with reference polysilicon. 4th International Conference on Silicon Photovoltaics, Silicon PV, Energy Procedia. 2014;602-607.
21. Berthod C, Strandberg R, Yordanov GH, Beyer HG, Odden JO. On the variability of the temperature coefficients of mc-Si solar cells with irradiance. 6th International Conference on Silicon Photovoltaics, Silicon PV, Energy Procedia, 2016, 2–9.
22. Dash PK, Gupta NC. Variation of temperature coefficient of different technology photovoltaic modules with respect to irradiance. *Int J Curr Eng Technol*. 2015;2347-5161. <http://inpressco.com/category/ijcet>
23. International Electrotechnical Commission (IEC). IEC 60904-7: 2019 Standard.
24. International Electrotechnical Commission (IEC). IEC TS 60904-1-2: 2019 Technical Specification.
25. Hishikawa Y, Yoshita M, Ohshima H, et al. Temperature dependence of the short circuit current and spectral responsivity of various kinds of crystalline silicon photovoltaic devices. *Jpn J Appl Phys*. 2018; 57(8S3):08RG17. <https://iopscience.iop.org/article/10.7567/JJAP.57.08RG17>

SUPPORTING INFORMATION

Additional supporting information may be found in the online version of the article at the publisher's website.

How to cite this article: Golve YR, Kottantharayil A, Vasi J, Shiradkar N. Determining the optimal standard test condition correction procedure for high-throughput field I-V measurements of photovoltaic modules. *Prog Photovolt Res Appl*. 2021;1-14. doi:10.1002/pip.3457